Available online at www.sciencedirect.com
ScienceDirect
Journal of Power Sources 168 (2007) 143–153
JOURNAL OF POWER SOURCES
www.elsevier.com/locate/jpowsour

In situ measurements of water crossover through the membrane for direct methanol fuel cells

C. Xu, T.S. Zhao *

Department of Mechanical Engineering, The Hong Kong University of Science and Technology, Clear Water Bay, Kowloon, Hong Kong SAR, China

Received 1 February 2007; received in revised form 7 March 2007; accepted 8 March 2007
Available online 15 March 2007

Abstract

We show analytically that the water-crossover flux through the membrane used for direct methanol fuel cells (DMFCs) can be in situ determined by measuring the water flow rate at the exit of the cathode flow field. This measurement method enables investigating the effects of various design and geometric parameters as well as operating conditions, such as properties of cathode gas diffusion layer (GDL), membrane thickness, cell current density, cell temperature, methanol solution concentration, oxygen flow rate, etc., on water crossover through the membrane in situ in a DMFC. Water crossover through the membrane is generally due to electro-osmotic drag, diffusion and back convection. The experimental data showed that diffusion dominated the total water-crossover flux at low current densities due to the high water concentration difference across the membrane. With the increase in current density, the water flux by diffusion decreased, but the flux by back convection increased. The corresponding net water-transport coefficient was also found to decrease with current density. The experimental results also showed that the use of a hydrophobic cathode GDL with a hydrophobic MPL could substantially reduce water crossover through the membrane, and thereby significantly increasing the limiting current as the result of the improved oxygen transport. It was found that the cell operating temperature, oxygen flow rate and membrane thickness all had significant influences on water crossover, but the influence of methanol concentration was negligibly small.

Keywords: Direct methanol fuel cells; Water crossover; Water management; Diffusion layer; Back convection

1. Introduction

The liquid-fed direct methanol fuel cell (DMFC), offering the tantalizing promise of cleaner electricity with less impact on the environment than traditional energy conversion technologies, has received much attention as a leading candidate power source for portable electronic devices, electric vehicles and other mobile applications. However, the commercialization of DMFCs is still hindered by several technological problems, among which the water management is one of the key issues [1–4]. Unlike in gas-hydrogen-fed polymer electrolyte fuel cells (PEFCs), in the DMFC, liquid methanol solution is fed to its anode. As a result, liquid water can transport, along with methanol, through the membrane from the aqueous anode to the cathode. Water crossover through the membrane may cause two problems for the DMFC technology. First, it results in a water loss from the anode, and thus make-up water is needed, especially for passive DMFCs [5,6]. Secondly, a high rate of water crossover increases the difficulty in avoiding the cathode-flooding problem, limiting the DMFC performance [5–11]. Therefore, suppressing water crossover through the membrane is beneficial not only for simplifying the DMFC system but also for improving cell performance. To this end, it is essential to gain a better understanding of the mechanisms of water crossover in DMFCs, which appears to be significantly different with that in PEFCs.

The study of water transport through Nafion membranes has been a focused interest over the past decade [5–33]. Ren et al. [7] experimentally determined the electro-osmotic drag coefficient of water in the ionomeric membrane used for a DMFC, and they found that the electro-osmotic drag coefficient increased with temperature. Rajalakshmi et al. [16] investigated water transport through the membrane used for a H_2/O_2 PEMFC by measuring the amount of product water at the anode side, and they found that

* Corresponding author. Tel.: +852 2358 8647; fax: +852 2358 1543.
E-mail address: metzhao@ust.hk (T.S. Zhao).

0378-7753/$ – see front matter © 2007 Elsevier B.V. All rights reserved.
doi:10.1016/j.jpowsour.2007.03.023

the water produced at the cathode could transport to the anode, thus allowing humidification for the anode gas and less condensed water in the cathode. Mennola et al. [17] studied the water balance in a free-breathing PEMFC, and the results showed that the rate of water crossover through the membrane depended on the operating temperature and the hydrogen flow rate, and the net-water transport coefficient varied across the whole electrode. Sandhu et al. [18] developed a mass flux model through the membrane used for a DMFC. They assumed that the membrane at the cathode side was always equilibrium with liquid water, and the predicted results showed that the water concentration at the cathode side of the membrane was slightly greater than that at the anode side, and thus water diffused from the cathode to the anode. Ge et al. [21] experimentally determined the electro-osmotic drag coefficient in a Nafion 117 membrane at different temperatures and water contents of the membrane. They also showed that the electro-osmotic drag coefficient of water in the Nafion membrane in contact with liquid water was independent of the cell current density. Schultz and Sundmacher [30] analyzed the methanol and water crossover through the membrane in a DMFC experimentally and theoretically. Contrary to the works of Sandhu et al. [18], they showed that the water concentration at the cathode side of the membrane was far less than that at the anode side, and diffusion was the major mode of water transport from the anode to the cathode through the membrane.

It has been understood that the cathode gas diffusion layer (GDL), which typically consists of a backing layer made of carbon paper or carbon cloth and a micro-porous layer (MPL), plays an important role on both water transport through the membrane and water ejection from the cathode. Recently, the effect of cathode GDL on water transport in PEFCs, including DMFCs, has been reported [5–11,28–33,15]. Peled et al. [5,6] developed a novel approach to recycle water and reduce water crossover in DMFCs, by building up high hydraulic pressure at the cathode with the use of a hydrophobic liquid water barrier layer. They showed that water crossover through the membrane could vary from negative, through zero, to positive values as a function of the thickness and properties of the water barrier layer. With the optimized water barrier layer, water losses could be minimized and a passive DMFC under water-neutral operation conditions was developed. Lu et al. [9] reported a novel DMFC design based on a thin Nafion 112 membrane and a GDL coated with a MPL. The hydraulic liquid pressure built up in the MPL resulting from the large MPL contact angle and small pore size was utilized to create the water back flow from the cathode to the anode, which substantially reduced water crossover through the membrane. Kim et al. [10] proposed a novel structure of membrane electrode assembly (MEA) for a passive DMFC. In the MEA, a hydrophilic anode GDL and a hydrophobic cathode GDL were used to enhance the water back flow through the membrane, while an additional hydrophilic diffusion layer was coated adjacent to the cathode catalyst layer (CL) to lower the water concentration difference across the membrane. Liu et al. [11] designed a novel MEA to attain lower rates of methanol crossover and water crossover and high cell performance simultaneously. The MEA also employed a highly hydrophobic cathode MPL to build up the hydraulic pressure at the cathode and hence drive the liquid water from the cathode to the anode to offset the water dragged by electro-osmosis. They also investigated the effect of different operating conditions, including current density, temperature, methanol concentration, etc.

Our literature review indicates that extensive efforts have been made for studying water transport through Nafion type of membranes used for DMFCs. However, most of previous studies have generally been limited to the cases without taking account the effects of MEA design and geometric parameters as well as operating conditions. A general understanding of water crossover through the membrane that is integrated with the MEA for DMFCs is far less understood. In this work, we present a theoretical analysis of water crossover through the entire MEA used for DMFCs, from which the net water-crossover flux through the membrane can be in situ determined. We show the water-crossover flux measured in an in-house fabricated DMFC with various MEA design and geometric parameters under different operating conditions.

2. Analytical

Water transport through the polymer electrolyte membrane used for PEFCs and DMFCs is generally due to three transport mechanisms: electro-osmotic drag by proton transport, diffusion by water concentration gradients and convection by hydraulic pressure gradients. We now focus on water crossover through the membrane in a liquid-fed DMFC by looking at the scenarios sketched in Fig. 1. Liquid water in the fed dilute methanol solution is transported from the anode channel through the GDL to the CL, where part of it reacts with methanol to form gas CO_2, while the remainder permeates through the membrane to the cathode. The permeated water, along with that produced from the oxygen-reduction reaction (ORR) on the cathode, is transported through the cathode CL and GDL to the cathode channel by the capillary pressure and is swept out from the channel by the oxygen/air flow stream. To quantify the total water-crossover

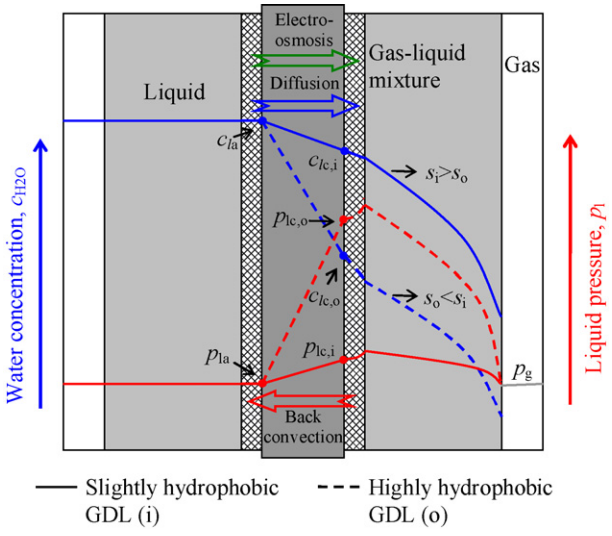

Fig. 1. Schematic illustrating water transport in a DMFC.

flux through the membrane in the DMFC, we first consider the water flux by electro-osmotic drag, which can be determined from:

$$J_{eo} = \kappa \frac{i}{F} \tag{1}$$

where κ is the electro-osmotic drag coefficient in the membrane, i the cell current density and F is Faraday's constant. The water crossover through the membrane is also by diffusion as a result of the water concentration (water content) difference across the membrane. The molar flux of water by diffusion can be determined from:

$$J_{diff} = D_{eff} \frac{c_{la} - c_{lc}}{\delta_m} \tag{2}$$

where D_{eff} is the effective diffusivity of water in the membrane, δ_m the membrane thickness, c_{la} and c_{lc} represent, respectively, liquid water concentrations at the anode and cathode surfaces of the membrane. From the phase equilibrium between the polymer and the free pores in CL [30], c_{la} is determined by the water saturation in the anode CL, which is influenced by the liquid water concentration and the rate of gas-CO_2 evolution in the CL that is related to cell current density. Similarly, c_{lc} is determined by the water saturation in the cathode CL, which is influenced by the rate of water generation at the cathode that is related to current density, by the water-crossover flux through the membrane, and by the rate of water removal from the GDL to the channel. In summary, the magnitude of both c_{la} and c_{lc} depends on the properties of the MEA, the flow field design and operating conditions. Under typical operating conditions without the cathode flooding (or at low current densities), it is expected that $c_{la} > c_{lc}$, leading to a positive diffusion flux (from the anode to the cathode). On the other hand, when the cathode is severely flooded (or at high current densities), very likely, the diffusion flux of water through the membrane becomes zero, as the membrane is fully hydrated on both sides. It is worth noting that among previous studies [7,9,12,18,30], the direction of diffusion flux of water is inconsistent.

The water flux by convection depends on the liquid pressure difference across the membrane, which can be determined from:

$$J_c = \frac{K\rho(p_{la} - p_{lc})}{\mu M_{H_2O}\delta_m} \tag{3}$$

where K is the permeability through the membrane, ρ the density of water, μ the viscosity of liquid water, M_{H_2O} the molecular weight of water, p_{la} and p_{lc} represent, respectively, liquid water pressure at the anode and cathode surfaces of the membrane. Since the velocity of liquid flow through the anode GDL is rather small, p_{la} is nearly the same as the liquid pressure in the anode flow channel. The liquid pressure at the cathode side p_{lc} can be related to the cathode gas pressure by the capillary pressure in the porous CL and GDL [34]:

$$p_c = p_g - p_{lc} = \sigma \cos\theta \left(\frac{\varepsilon}{K_d}\right)^{1/2} J(s) \tag{4}$$

where p_g is the gas pressure at the cathode, σ the surface tension, K_d the permeability of the GDL, ε the porosity of the GDL, θ the contact angle (>90° for hydrophobic porous media) and $J(s)$ is the Leverette function which is always positive and is a function of liquid fraction in the porous electrode. Typically, the DMFC operates at the same pressure on both the anode and the cathode, i.e. $p_g = p_{la}$. Thus, substituting Eq. (4) into Eq. (3), we obtain:

$$J_c = \frac{K\rho\sigma\cos\theta}{\mu M_{H_2O}\delta_m} \left(\frac{\varepsilon}{K_d}\right)^{1/2} J(s) \tag{5}$$

The above equation indicates that even though the DMFC operates at the same pressure on both the anode and cathode, a hydrophobic GDL ($\cos\theta < 0$) may cause a convection from the cathode to the anode (i.e. $J_c < 0$), which is termed as 'back convection' hereafter. Eq. (5) also implies that the back-convection flux increases with the hydrophobic level ($\theta > 90°$) and the water-saturation level of the GDL [34].

In summary, the total water-crossover flux through the membrane can be obtained by summing up Eqs. (1), (3) and (5) to give:

$$J_{wc} = J_{eo} + J_{diff} + J_{bc} = \alpha \frac{i}{F} \tag{6}$$

where α represents the so-called net water-transport coefficient. Clearly, the net water-transport coefficient is influenced by all the parameters that affect J_{eo}, J_{diff} and J_{bc}, such as the geometric dimensions and properties of the membrane, CL and GDL. Note that in Eq. (6), the sign of J_{bc} is in opposition to J_{eo} and J_{diff}. Hence, the net water-crossover flux through the membrane can be reduced by utilizing the back convection to offset the flux of water by electro-osmotic drag and diffusion [5–11]. The increase in the flux by back convection and the decrease in the flux by diffusion can be achieved by optimizing the MEA design. It has been demonstrated that it is possible to achieve a zero net flux of water crossover through the membrane (a neutral water balance) by properly designing the MEA [5].

With the water-crossover flux through the membrane given by Eq. (6), we can now consider the water transport from the cathode CL to the flow channel. Under steady state, the total molar flux of water from the cathode CL to the flow channel can be expressed as:

$$\frac{N_{H_2O}}{A} = J_{ORR} + J_{MOR} + J_{wc} \tag{7}$$

where A is the electrode area and N_{H_2O} is the water flow rate collected at the cathode channel exit. J_{ORR} and J_{MOR} represent, respectively, the molar flux of water due to the ORR and MOR, which are given by:

$$J_{ORR} = \frac{i}{2F} \tag{8}$$

and

$$J_{MOR} = \frac{i_c}{3F} \tag{9}$$

where i_c is the equivalent methanol-crossover current density. Assuming that methanol crossover through the membrane depends on electro-osmosis and diffusion, the equivalent

methanol-crossover current density can be deduced to give (see Appendix A for more details):

$$i_c = i_{c,ocv}\frac{1+(ai/Fk_m)}{1+(ai/F(k_m+k_d))}\left(1-\frac{i}{i_{lim}}\right) \quad (10)$$

where $i_{c,ocv}$ represents the equivalent methanol-crossover current density at the open-circuit voltage (OCV), i_{lim} the anode liming current density caused by the methanol transport limitation, a a constant related to the electro-osmotic drag coefficient, k_d the effective mass-transport coefficient from the channel to the anode CL, k_m the effective mass-transport coefficient through the membrane; k_b can be determined by measuring the anode limiting current density with low methanol concentration and using the following expression [4]:

$$k_b = \frac{i_{lim}/6F}{c_{in}-(i_{lim}A/12FQ)} \quad (11)$$

where Q is the methanol solution flow rate. Alternatively, for the given k_b and c_{in}, the anode limiting current density at high methanol concentrations can also be approximated by Eq. (11). k_m can be approximated from the methanol balance equation at open-circuit condition and using the measured methanol crossover ($i_{lim,c}$) at low methanol concentration (e.g. 0.25 M):

$$i_{lim,c} = \frac{6Fc_{in}}{(1/k_d)+(1/k_m)} \quad (12)$$

With this approximated k_m, the measured $i_{lim,c}$ can be finally modified to be the oxidation current of the total methanol crossover from the anode to the cathode at open-circuit condition accounting for the electro-osmotic drag effect [35]

$$i_{c,ocv} = i_{lim,c}\frac{6\kappa(k_d x_{in}/(k_d+k_m))}{\ln(1+6\kappa(k_d x_{in}/(k_d+k_m)))} \quad (13)$$

where x_{in} is the molar fraction of methanol in the fed methanol solution.

From Eq. (7) and with the aid of Eqs. (8)–(10), we can obtain:

$$J_{wc} = \frac{N_{H_2O}}{A}-\frac{i}{2F}-\frac{i_c}{3F} = \frac{N_{H_2O}}{A}-i\left(\frac{1}{2F}+\frac{1}{3F}\frac{1+(ai/Fk_m)}{1+(ai/F(k_m+k_d))}\left(\frac{i_{c,ocv}}{i}-\frac{i_{c,ocv}}{i_{lim}}\right)\right) \quad (14)$$

It follows that the net water-transport coefficient can be determined from:

$$\alpha = \frac{J_{wc}F}{i} = \frac{N_{H_2O}F}{Ai}-\left(\frac{1}{2}+\frac{1}{3}\frac{1+(ai/Fk_m)}{1+(ai/F(k_m+k_d))}\left(\frac{i_{c,ocv}}{i}-\frac{i_{c,ocv}}{i_{lim}}\right)\right) \quad (15)$$

Eqs. (14) and (15) indicate that once the relevant mass-transport parameters (A, a, k_m, k_d, i_{lim}, $i_{c,ocv}$) are known, the total molar flux of water crossover through the membrane in a DMFC and the corresponding net water-transport coefficient can be in-situ determined by measuring the water flow rate at the cathode channel exit at a given cell current density. With Eqs. (14) and (15), the effects of various parameters, such as methanol concentration, cell temperature, type of GDL, membrane thickness, oxygen flow rate and others, on the water-crossover flux and the net water-transport coefficient can be investigated systematically.

3. Experimental

3.1. The DMFC

The in-house fabricated DMFC consisted of a MEA, with an active area of 2.0 cm × 2.0 cm, sandwiched between two bipolar plates, which were fixed by two fixture plates. The MEA consisted of a Nafion 112 (or 117) membrane and two electrodes. Unless mentioned otherwise, the anode electrode was a single-side ELAT electrode from E-TEK, which used carbon cloth (E-TEK, type A) with 30 wt% PTFE wet-proofing treatment as the backing layer. 4.0 mg cm^{-2} unsupported Pt/Ru (1:1 atom%) was used as the catalyst on the anode. On the cathode, the CL was fabricated in-house by the decal method [36,37]. The catalyst ink was prepared by the method reported elsewhere [36,37] and sprayed onto the Teflon blank. The CL was then transferred onto the membrane by hot pressing the catalyst coated Teflon blank and the anode electrode on the two sides of the membrane at 135 °C and 4.0 MPa for 3 min. The cathode catalyst loading was about 2.0 mg cm^{-2} using 60% Pt on Vulcan XC-72 from E-TEK. The content of Nafion ionomer in the cathode CL was maintained to be about 20 wt%. Three different cathode GDLs were tested in the experiments, including untreated Toray-090 carbon paper, 30 wt% PTFE treated Toray-090 and 30 wt% PTFE treated Toray-090 with a hydrophobic MPL. The MPL applied on the carbon paper consisted of Vulcan XC-72 carbon powder and 30 wt% PTFE, with a total loading about 2.0 mg cm^{-2}. The decal method for preparing the cathode ensured that the effect of cathode GDL be investigated using different cathode GDLs for the same cathode CL, the same membrane and the same anode.

For convenience of temperature control, both the anode and cathode fixture plates were made of stainless-steel blocks. Single serpentine flow fields, having 0.8 mm channel width, 1.2 mm rib width and 0.8 mm depth, were formed in the fixture plates for both the anode and cathode sides.

3.2. Measurement instrumentation and test conditions

The experiments were carried out in the test rig detailed elsewhere [3]. On the anode, aqueous methanol solution was fed by a digital HPLC micro-pump (Series III). Before entering the cell, methanol solution was pre-heated to a desired temperature by a heater connected to a temperature controller. On the cathode, 99.999% high purity oxygen was supplied without humidification. A mass flow meter (Omega FMA-7105E), along with a multiple channel indicator (Omega FMA-5876A),

was used to control and measure the flow rate of oxygen. The Arbin BT2000 (Arbin Instrument) electro-load interfaced with a computer was employed to control the cell operation and measure voltage–current (polarization) curves. The experiments were performed at different temperatures and fed with pure oxygen with different flow rates. Methanol concentration was varied from 1.0 to 4.0 M, while the flow rate was fixed at 2.0 ml min^{-1}. At such a relatively high flow rate of methanol solution, the methanol consumption along channel length is so small such that methanol concentration can be assumed to be uniform from the inlet to outlet. To measure the anode limiting current density (i_{lim}) at low methanol concentration, 0.25 and 0.5 M methanol solution were used, and a high oxygen flow rate was used to ensure that the measured limiting current density of the DMFC was caused only by the mass-transport limitation of methanol [4]. The rate of methanol crossover $i_{lim,c}$ was measured by the voltammetric method [35]. Methanol solution at the flow rate of 2.0 ml min^{-1} was fed into the anode, while liquid water, at the same flow rate, was fed into the cathode to create an inert atmosphere. When a positive voltage of 0.85 V was applied on the cathode, the limiting current density $i_{lim,c}$ could be measured. A water trap filled with Dryerite® (anhydrous $CaSO_4$) was connected to the exit of the cathode channel to collect the water. The water was collected by maintaining a constant current density for about 0.5–3 h. Fifteen minutes were usually needed to make the operating point to be stabilized at every water-collecting point. To eliminate the influence of back pressures on the water transport through the membrane, the respective back pressures on the anode and cathode compartments were kept to the atmosphere pressure. The measured mass-transport parameters are listed in Table 1.

Table 1
Measured mass transport parameters used to determine the water-crossover flux

Mass transport parameters	Values
For cathode CCM with Nafion 112	
k_b @ 70 °C	0.75×10^{-5} m s^{-1}
k_b @ 50 °C	0.35×10^{-5} m s^{-1}
k_b @ 30 °C	0.17×10^{-5} m s^{-1}
k_m @ 70 °C	1.32×10^{-5} m s^{-1}
k_m @ 50 °C	0.64×10^{-5} m s^{-1}
k_m @ 30 °C	0.31×10^{-5} m s^{-1}
i_c @ 1.0 M, 70 °C	282.7 mA cm^{-2}
i_c @ 2.0 M, 70 °C	568.1 mA cm^{-2}
i_c @ 4.0 M, 70 °C	1068 mA cm^{-2}
i_c @ 1.0 M, 50 °C	114.6 mA cm^{-2}
i_c @ 1.0 M, 30 °C	72.1 mA cm^{-2}
κ	$-1.834 + 0.0126T$ [21]
For cathode CCM with Nafion 117	
k_b @ 70 °C	0.75×10^{-5} m s^{-1}
k_m @ 70 °C	0.354×10^{-5} m s^{-1}
i_c @ 2.0 M, 70 °C	225.4 mA cm^{-2}
For anode CCM with untreated GDL	
k_b @ 70 °C	1.59×10^{-5} m s^{-1}
k_m @ 70 °C	0.66×10^{-5} m s^{-1}
i_c @ 1.0 M, 70 °C	279.7 mA cm^{-2}
For anode CCM with PTFE-treated GDL	
k_b @ 70 °C	1.26×10^{-5} m s^{-1}
k_m @ 70 °C	0.544×10^{-5} m s^{-1}
k_m @ 1.0 M, 70 °C	223.8 mA cm^{-2}

4. Results and discussion

4.1. General behavior

Fig. 2 shows the variation in the water flux measured at the cathode channel exit, N_{H_2O}/A (represented by circle symbols),

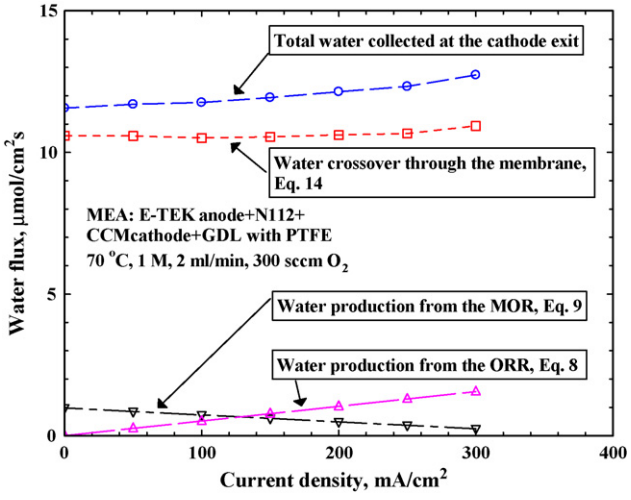

Fig. 2. Variation in the water flux collected at the cathode channel exit with current density.

with current density. The DMFC was operated at 70 °C and fed with 1.0 M-methanol solution at the flow rate of 2.0 ml min^{-1} and pure oxygen at the flow rate of 300 sccm. The MEA consisted of the Nafion 112 membrane and PTFE-treated carbon paper as the cathode GDL, noting that the anode GDL was made of 30 wt% PTFE treated carbon cloth for all the experiments. As expected, the water flux at the cathode channel exit increased gradually with current density. Also shown in Fig. 2, are the flux of water production by the ORR, J_{ORR} (represented by upward triangles), calculated from Eq. (8), and by the MOR, J_{MOR} (represented by downward triangles), calculated from Eq. (9). It is interesting to notice that the flux of water production by each reaction was substantially lower than the total water flux measured at the cathode channel exit. However, the water-crossover flux through the membrane, J_{wc} (represented by square symbols), which was determined from Eq. (14), was very much close to N_{H_2O}/A. The substantially smaller difference between N_{H_2O}/A and J_{wc} as well as the larger difference between N_{H_2O}/A and the sum of J_{ORR} and J_{MOR} suggest that the total molar flux of water collected at the cathode channel exit be predominated by water crossover through the membrane (up to 92%). The higher flow rate of water crossover not only results in a water loss from the anode but also causes the cathode to be flooded if water cannot be effectively removed from the cathode. Therefore, unlike the water management in H_2/O_2 PEFCs, the water management in DMFCs is to reduce the rate of water crossover or increase the water-transport limitation on the cathode so that the electrode flooding problem can be avoided. Another interesting observation can be made from Fig. 2 is that

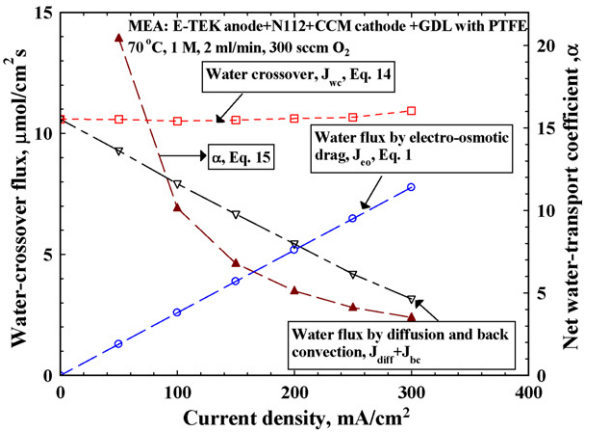

Fig. 3. Variation in the water-crossover flux through the membrane and the corresponding net water-transport coefficient with current density.

the increase in the water-crossover flux, J_{wc}, with current density was rather slow. This finding is consistent with that by Schultz and Sundmacher [30].

Let us now examine how the water flux by each water-transport mechanism in the membrane varied with current density by studying Fig. 3. First, it is seen that the water flux by electro-osmotic drag, J_{eo} (represented by circles), increased linearly with current density, which was plotted based on Eq. (1). Secondly, look at the curve (open triangles) representing the water flux by the combined effect of diffusion and back convection, $J_{diff} + J_{bc}$, which was obtained from $J_{wc} - J_{eo}$. The following observations can be made from the curve representing $J_{diff} + J_{bc}$. First, since J_{bc} was always negative (from the cathode to the anode), the positive values of $J_{diff} + J_{bc}$ indicate that the water flux by diffusion from the anode to the cathode was always larger than that by back convection. This fact suggests that under typical operating conditions the water concentration at the anode, c_{la}, be higher than that at the cathode, c_{lc}, perhaps meaning that the cathode is not flooded. Hence, previous treatments in modeling DMFCs by assuming a uniform water content across the membrane will cause significant errors in predicting cell performance. Secondly, it is observed from Fig. 3 that $J_{diff} + J_{bc}$ was rather sensitive to the change in current density: $J_{diff} + J_{bc}$ was reduced from about 10.5 to 3.5 μmol cm^{-2} s^{-1} when current density was increased from 0 to 300.0 mA cm^{-2}. This rapid decrease in $J_{diff} + J_{bc}$ with current density was the consequence of a sharp decrease in J_{diff} and an increase in J_{bc}. For the diffusion effect, as illustrated in Fig. 1, water concentrations at both the anode, c_{ac}, and the cathode, c_{lc}, of the membrane were influenced by current density. On the anode, the rate of gas CO_2 production increased with current density. As a result, the liquid fraction in the anode CL decreased with current density. Hence, c_{la} decreased with current density. While on the cathode, both the water flux by electro-osmotic drag J_{eo} and the rate of water production increased with current density. As a result, c_{lc} increased with current density. Thus, the decrease in c_{la} and the increase in c_{lc} resulted in a reduction in J_{diff} with current density. For the back convection effect, higher water saturation in the cathode CL also led to higher liquid saturation in the cathode GDL. As a result, the capillary pressure increased with current density, resulting in a larger water flux by back convection J_{bc}. Therefore, the opposite variations in J_{diff} and J_{bc} with current density led to the behavior that $J_{diff} + J_{bc}$ rapidly decreased with current density.

Fig. 3 also shows the corresponding net water-transport coefficient, α (represented by upward triangles), which was determined from Eq. (15). It is seen that α decreased rapidly at low current densities, but the decrease became slower at high current densities, from about 20.5 to 3.7 when current density was increased from 50.0 to 300.0 mA cm^{-2}. This variation trend of α is consistent not only with that measured in a PEFC [32] but also with that in a DMFC [11]. It should be noted that the value of α in Fig. 3 was much larger than the electro-osmotic drag coefficient in the Nafion membrane, about 2.48 at 70 °C, as shown in Table 1. This implies that the water flux by back convection in this MEA was insufficient to offset that by diffusion. The rapid change in α with current density shown in Fig. 3 also suggests that the comparison in the rate of water crossover by α between different MEAs have to be made at the same current density.

As discussed above, the increase in the rate of gas CO_2 production with current density can decrease the water flux by diffusion through the membrane. To verify this point, the rate of water crossover was measured for two MEAs that consisted the same membrane (Nafion 112) and the same cathode (a commercial single-side ELAT cathode from E-TEK) but different anode GDLs: one was made of a untreated Toray-090 carbon paper whereas the other was made of 30 wt% PTFE-treated Toray-090 carbon paper. The measured water-crossover flux for the two different anode GDLs are shown in Fig. 4. The water crossover was larger for the untreated GDL, and the difference became larger with the increase of current density. This difference was obviously caused by the difference in J_{diff} between the two anode GDLs. It is well understood that at a given current density, the CO_2 gas fraction in the GDL is increased with the increase of hydrophobic level of the GDL. Accordingly, c_{la} was lower for the anode GDL with higher hydrophobic level, resulting in a lowered J_{diff} and thus the lower flux of water crossover. This result clearly proves the considerable influence of anode CO_2 evolution on the water crossover through the membrane.

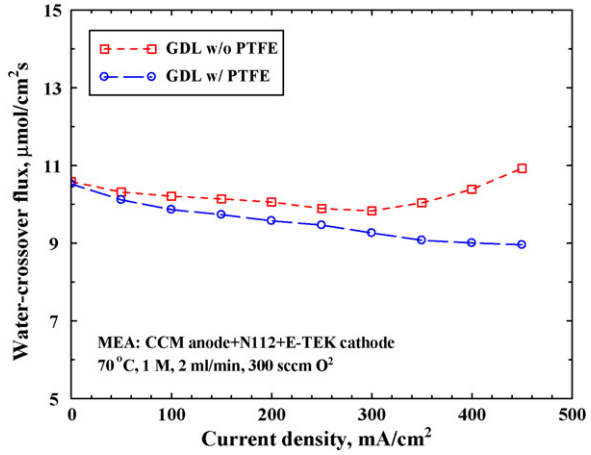

Fig. 4. Effect of anode GDL on the water-crossover flux through the membrane.

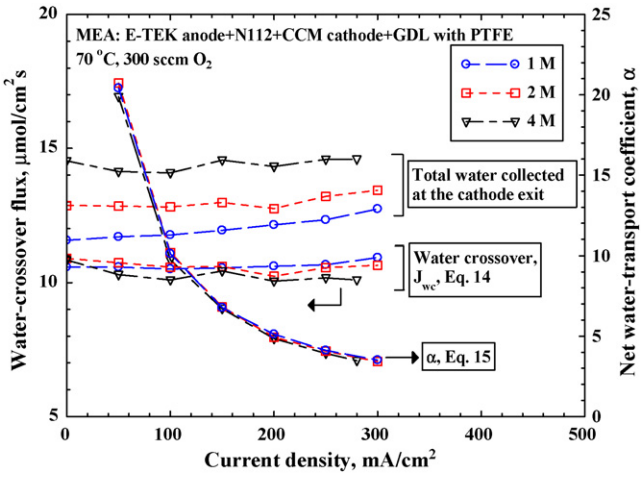

Fig. 5. Effect of methanol concentration on the water-crossover flux and the net water-transport coefficient.

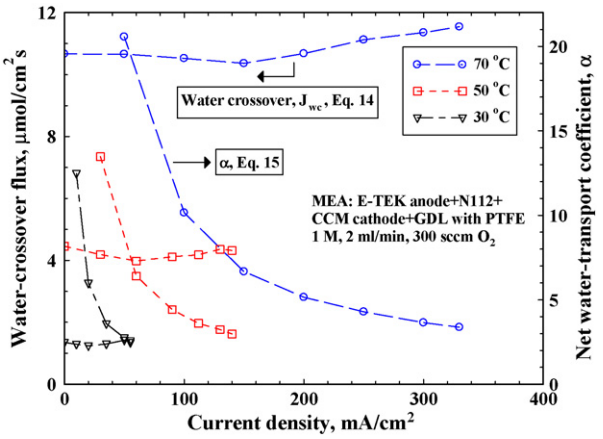

Fig. 6. Effect of cell temperature on the water-crossover flux and the net water-transport coefficient.

4.2. Effect of methanol concentration

Methanol solutions with different methanol concentrations, i.e. 1.0, 2.0 and 4.0 M, were tested to study its effect on water crossover; the results are shown in Fig. 5. The total water flux N_{H_2O}/A measured at the cathode channel exit was enlarged by about 25% when methanol concentration was increased from 1.0 to 4.0 M. However, it is interesting to see from Fig. 5 that the water-crossover fluxes for different methanol concentrations were almost the same. Thus, the higher water flux measured at the cathode channel exit for higher methanol concentration must have come from the increased water production from the MOR associated with the increased methanol crossover. As a result, the corresponding net water-transport coefficients nearly coincided with each other for different methanol concentrations, as shown in Fig. 5. In summary, the experiments showed that the methanol concentration had a negligible influence on the water-crossover flux through the membrane.

4.3. Effect of temperature

To investigate the effect of temperature on water crossover, experiments were conducted at three different temperatures (i.e. 30, 50 and 70 °C); the results are shown in Fig. 6. It is seen that the water-crossover flux increased substantially with temperature: when temperature was increased from 30 to 70 °C, the water-crossover flux increased from about 1.4 to 10.7 μmol cm^{-2} s^{-1}. From Eq. (6), it is understood that the increased water-crossover flux was caused by the increased water diffusivity, electro-osmotic drag coefficient and permeability at elevated temperatures. The corresponding net water-transport coefficient was also dependent on temperature. Although α always decreased rapidly at low current densities and the decrease became slower at high current densities at all temperatures, it significantly increased with temperature at a given current density. For example, at the current density of 60.0 mA cm^{-2}, α increased from about 6.4 to 18.5 when temperature was increased from 50 to 70 °C. This trend is consistent with that by Liu et al. [11]. Therefore, α depended on the two variables: temperature and current density. One should investigate the effect of temperature on α with the same current density. However, it should be mentioned that the operating current density is usually low at low cell temperatures, and investigations of the temperature effect on α using different current densities for different temperatures have been reported by several researches [5,6,9,11]. This may lead to incorrect conclusions. For example, 30.0 mA cm^{-2} at 30 °C, 80.0 mA cm^{-2} at 50 °C and 200.0 mA cm^{-2} at 70 °C all corresponded to the same $\alpha = 5.0$, but this does not mean that the temperature had no influence on water crossover.

4.4. Effect of cathode GDL

We first investigated the hydrophobic level of cathode GDL on cell performance and water crossover. Two carbon papers with different hydrophobic levels were used as the cathode GDL in the experiments: one was the as-received untreated carbon paper that was slightly hydrophobic, while the other was 30 wt% PTFE-treated carbon paper that was highly hydrophobic. We also investigated the effect of the hydrophobic MPL by comparing the performance with different cathode GDLs: 30 wt% PTFE-treated carbon paper with and without a MPL. The results of cell performance and water crossover are shown in Figs. 7 and 8, respectively. It is seen from Fig. 7 that the DMFC with the three different cathode GDLs yielded nearly the same voltages at low current densities, implying that the voltage differences at high current densities were mainly caused by the different cathode GDLs.

Let us first examine the polarization curves corresponding to the PTFE-treated GDL and the untreated GDL, shown in Fig. 7. It is found that the PTFE-treated GDL showed a significantly lower mass-transport limitation than did the untreated GDL, indicating that the oxygen-transport resistance became larger after the carbon paper was PTFE treated. This phenomenon was also found in PEFCs [28,29]. This seems contradictory to the original purpose of PTFT treating carbon papers to reduce the oxygen transport resistance. Actually, it has already been found that PTFE in a carbon paper is prone to form thin films, which

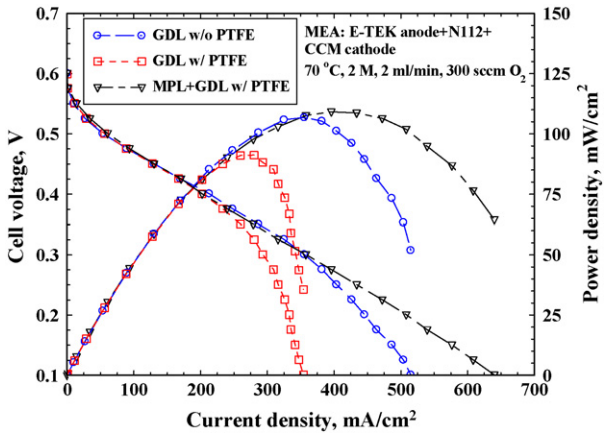

Fig. 7. Polarization curves with different cathode GDLs.

may block the gas pores and cause a larger gas-transport resistance [28–33,15,34–36]. This fact suggests that PTFE treatment be carefully processed such that a proper hydrophobicity can be achieved but severe gas pore blockages can be avoided.

As shown in Fig. 8, the water-crossover flux was significantly reduced, from about 15.0 to 11.0 μmol cm^{-2} s^{-1}, after the carbon paper was PTFE treated. Correspondingly, the net water-transport coefficient was also reduced as a result of using the PTFE-treated carbon paper: i.e. α decreased from about 7.0 to 5.0 at the current density of 200.0 mA cm^{-2}. This clearly indicates that although PTFE in carbon papers may increase the oxygen-transport resistance by pore blocking, the increased hydrophobicity can indeed help to reduce the water-crossover flux through the membrane. The lower water-crossover flux with the PTFE-treated carbon paper must be associated with the increase in J_{bc}. The increase in J_{bc} as a result of the increased hydrophobicity of the cathode GDL can be understood by examining Eq. (5), which indicates that the liquid pressure at the cathode increases with the hydrophobicity of cathode GDL. As illustrated in Fig. 1, the liquid pressure at the cathode side is increased from $p_{lc,i}$ to $p_{lc,o}$ after using the PTFE-treated GDL. Hence, the use of the PTFE-treated cathode GDL can enhance back convection J_{bc} from the cathode to the anode.

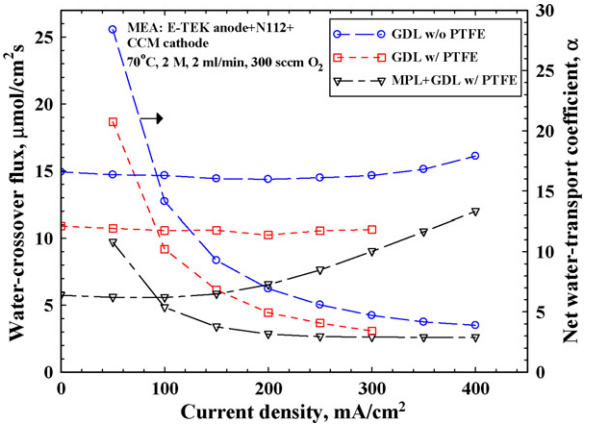

Fig. 8. Effect of cathode GDL on the water-crossover flux and the net water-transport coefficient.

When a hydrophobic MPL was applied onto the PTFE-treated GDL, it can be seen in Fig. 7 that the mass-transport limitation was increased from about 350.0 mA cm^{-2} to more than 650.0 mA cm^{-2}, which indicates that the oxygen-transport resistance was significantly reduced by adding the MPL. Since the GDLs all consisted of the PTFE-treated carbon papers and a MPL also functioned as an additional oxygen-transport resistance, the improved oxygen transport through the GDL with a MPL indicates that water flooding in the GDL was effectively mitigated after adding the MPL. This is coincident with the results of water crossover shown in Fig. 8, where it can be seen that the water-crossover flux was further markedly reduced after adding the MPL, and in particular, at low current densities the water-crossover flux was reduced from about 11.0 to 6.0 μmol cm^{-2} s^{-1}. As a result, the corresponding α decreased, i.e. from about 5.0 to 3.0 for the current density of 200.0 mA cm^{-2}. Therefore, the results show that the hydrophobic MPL helped to significantly reduce water crossover and thus mitigate the water accumulation in the GDL, thereby effectively improving the oxygen transport in the cathode. The reduced water crossover was also caused by the enhancement of J_{bc}. Eq. (4) indicates that a very large capillary pressure can be induced by the MPL [5,34], since the pores in the MPL are much smaller than that in carbon papers. As a result, a larger liquid pressure can enhance J_{bc} and significantly reduce the water-crossover flux. The hydrophobic MPL has been successfully utilized to lower the water crossover and even achieve neutral or reverse water transport [5,6,9,11]. In summary, in general the use of a PTFE-treated cathode GDL can reduce the water-crossover flux, but the PTFE loading to carbon papers cannot be too high as PTFE films formed in gas pores may increase the oxygen-transport resisitance. On the other hand, the MPL plays a more significant role on both the water crossover and oxygen transport.

4.5. *Effect of oxygen flow rate*

To prevent cathode flooding in DMFCs, a sufficiently high oxygen flow rate is usually required to sweep out liquid water in the cathode channel and GDL. The water-crossover flux under open-circuit conditions was measured with different cathode GDLs and by varying the oxygen flow rate from 60 to 480 sccm; the results are shown in Fig. 9. It is seen that for all the cathode GDLs the water-crossover flux increased with the oxygen flow rate, and particularly, the GDL without PTFE treatment exhibited much more rapid increase in the water-crossover flux with oxygen flow rate than did the other two cases. An increase in oxygen flow rate reduced the water fraction in the GDL, which led to a lowered water concentration c_{lc} and a lowered liquid pressure p_{lc} at the cathode surface of the membrane. The increase in J_{diff} and decrease in J_{bc} resulted in an increase in the water-crossover flux through the membrane. The reduced water fraction in the GDL by increasing the oxygen flow rate can be proved by observing the polarization curves shown in Fig. 10. It can be seen that for the GDL with PTFE treatment the limiting current density increased nearly three times (from about 132.0 to 384.0 mA cm^{-2}) when the oxygen flow rate was increased from 60 to 300 sccm.

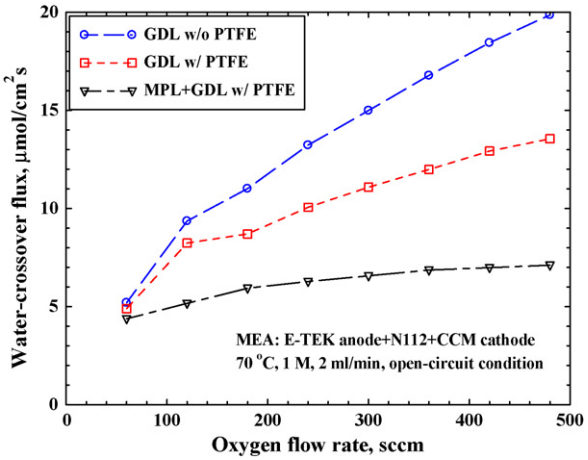

Fig. 9. Effect of oxygen flow rate on the water-crossover flux at open-circuit condition and with different cathode GDLs.

Similar to Fig. 8, Fig. 9 also indicates that the use of the PTFE-treated GDL and the addition of the MPL can substantially reduce the water-crossover flux through the membrane.

4.6. Effect of membrane thickness

The water-crossover fluxes through two membranes (Nafion 112 and 117) with the cathode GDL consisting of either the PTFE-treated GDL or the untreated one are compared in Fig. 11. It can be seen that for the same cathode GDL, the water-crossover flux through the thicker membrane was much lower than through the thinner one. For example, for the untreated GDL, the water crossover was reduced from about 15.0 to 12.2 μmol cm^{-2} s^{-1} when Nafion 112 was replaced with the Nafion 117 membrane. Eqs. (2) and (3) indicate that an increase in membrane thickness will result in a decrease in both J_{diff} and J_{bc}, and thus a lowered water-crossover flux. More importantly, it can be seen from Fig. 11 that for the thinner membrane (Nafion 112), the use of the PTFE-treated GDL resulted in a decrease in the water-crossover flux by about 4.0 μmol cm^{-2} s^{-1}, but the use of the PTFE-treated GDL in combination with the thicker membrane (Nafion 117) led to a decrease in the water-crossover flux by about 3.2 μmol cm^{-2} s^{-1} only. This comparison suggests that reducing water crossover by enhancing back convection be more effective with the use of thin membranes.

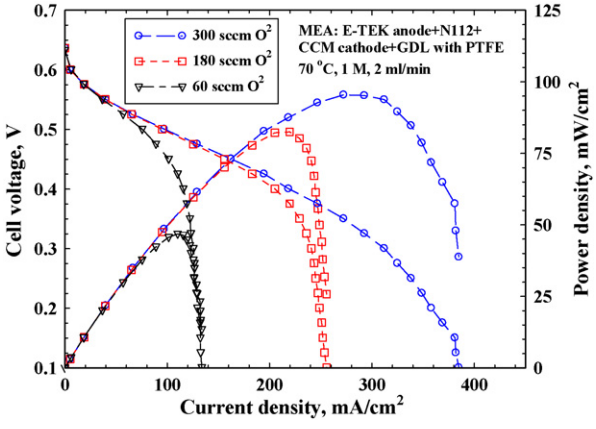

Fig. 10. Polarization curves with different oxygen flow rates.

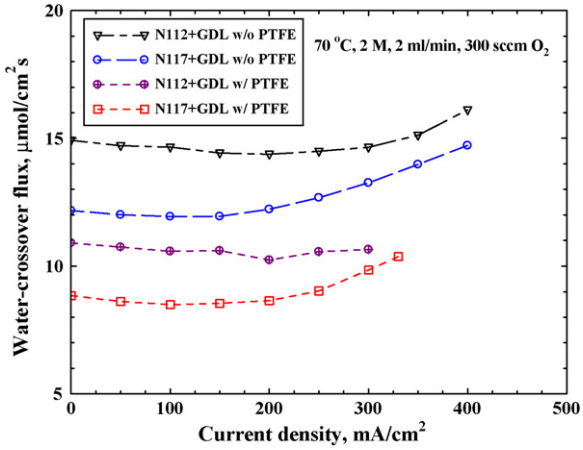

Fig. 11. Effect of membrane thickness on the water-crossover flux with different cathode GDLs.

5. Conclusions

Reducing the water transport from the anode to the cathode through the membrane is of significant importance for the water management in DMFCs, and thus it is critical to gain a better understanding of the mechanism of water crossover through the membrane used for DMFCs. In this work, we have shown analytically that the water-crossover flux through the membrane can be in situ determined by measuring the water flow rate at the exit of the cathode flow field. We have further demonstrated that this in situ method enables us to investigate the effects of various design and geometric parameters of the MEA and operating conditions, such as properties of GDLs, membrane thickness, cell current density, operating temperature, methanol solution concentration and oxygen flow rate, on water crossover through the membrane used in DMFCs. Salient findings and conclusions, which are valuable in the development of models for predicting water transport in operating DMFCs, are summarized as follows:

(1) Water crossover through the membrane is in general due to electro-osmotic drag, diffusion and back convection. The experimental results showed that at low current densities diffusion dominated the total water-crossover flux. With the increase in current density, the water flux by diffusion decreased significantly, whereas the flux by back convection increased to some extent. Accordingly, the net water-transport coefficient decreased rapidly at low current densities, but the decrease became slower at high current densities. The rapid change in the net water-transport coefficient with current density suggests that the comparison in the water-crossover flux between different MEAs have to be made at the same current density.
(2) Increasing the hydrophobic level of the cathode GDL could significantly lower the water-crossover flux as the result of

the enhanced back convection. In particular, the addition of a hydrophobic MPL to the cathode GDL could greatly enhance back convection and thus substantially suppress water crossover through the membrane. Consequently, the use of the hydrophobic cathode GDL with a hydrophobic MPL enables the electrode water-flooding problem to become less serious, and thereby significantly increasing the limiting current as the result of the improved oxygen transport.

(3) It was found that the cell operating temperature, oxygen flow rate and membrane thickness all had significant influences on water crossover, but the influence of methanol concentration was negligibly small. At a given current density, the water-crossover flux increased with temperature but decreased with membrane thickness. An increase in oxygen flow rate markedly increased the water-crossover flux through the membrane. The results also showed that reducing water crossover by enhancing back convection was more effective with the use of thin membranes.

Acknowledgement

The work described in this paper was fully supported by a grant from the Research Grants Council of the Hong Kong Special Administrative Region, China (Project No. 622706).

Appendix A. Deduction of the methanol-crossover current

At the DMFC anode, methanol is transported from the channel through the gas diffusion layer (GDL) to the electrode, where part of it is oxidized and the remainder is transported through the membrane to the cathode side. From the mass balance, assuming all the permeated methanol will be oxidized in the cathode catalyst layer (CL) (or zero methanol concentration), we have

$$k_d(c_{in} - c_{cl}) = \frac{i}{6F} + \frac{i_c}{6F} \tag{A-1}$$

where c_{in} is the methanol concentration in the channel, c_{cl} the methanol concentration in the anode CL, i the current density, i_c the methanol-crossover current density, k_d the effective mass transport coefficient from the channel to the CL and k_m is the mass transport coefficient through the membrane. Thus, at the liming current density, i.e. $c_{cl} = 0$, the equation can be reduced to:

$$i_{lim} = 6Fk_d c_{in} \tag{A-2}$$

The methanol-crossover current density as the result of both diffusion and electro-osmotic drag can be expressed as:

$$\frac{i_c}{6F} = k_m c_{cl} + \kappa x_{cl}\frac{i}{F} \approx k_m c_{cl} + \kappa\frac{c_{cl}}{(1000/0.018)}\frac{i}{F} = \left(k_m + a\frac{i}{F}\right)c_{cl} \tag{A-3}$$

where κ is the electro-osmotic drag coefficient of water and the constant $a = 1.8e-5\kappa$. Under the open-circuit condition ($i = 0$), combining Eqs. (A-2) and (A-3) gives:

$$\frac{i_{c,ocv}}{6F} = k_m c_{cl,ocv} = k_d(c_{in} - c_{cl,ocv}) = \frac{k_m k_d}{k_m + k_d}c_{in} \tag{A-4}$$

Solving c_{cl} from Eqs. (A-1)–(A-3), we obtain:

$$c_{cl} = \frac{i_{lim} - i}{6F(k_d + k_m + a(i/F))} \tag{A-5}$$

Substituting Eq. (A-5) into (A-3), and with the help of Eqs. (A-2) and (A-4), the equivalent methanol-crossover current density can finally be expressed as:

$$i_c = i_{c,ocv}\frac{(1 + (ai/Fk_m))}{1 + (ai/F(k_m + k_d))}\left(1 - \frac{i}{i_{lim}}\right) \tag{A-6}$$

References

[1] J. Larmine, A. Dicks, Fuel Cell Systems Explained, second edn., Wiley, Chichester, West Sussex, 2003.
[2] C. Xu, T.S. Zhao, Electrochem. Commun. 9 (2007) 493.
[3] H. Yang, T.S. Zhao, Q. Ye, J. Power Sources 139 (2005) 79.
[4] C. Xu, Y.L. He, T.S. Zhao, R. Chen, Q. Ye, J. Electrochem. Soc. 153 (2006) A1358.
[5] E. Peled, A. Blum, A. Aharon, M. Philosoph, Y. Lavi, Electrochem. Solid-State Lett. 6 (2003) A268.
[6] A. Blum, T. Duvdevani, M. Philosoph, N. Rudoy, E. Peled, J. Power Sources 117 (2003) 22.
[7] X. Ren, W. Henderson, S. Gottesfeld, J. Electrochem. Soc. 144 (1997) L267.
[8] G.Q. Lu, C.Y. Wang, J. Power Sources 134 (2004) 33.
[9] G.Q. Lu, F.Q. Liu, C.Y. Wang, Electrochem. Solid-State Lett. 8 (2005) A1.
[10] H. Kim, J. Oh, J. Kim, H. Chang, J. Power Sources 162 (2006) 497.
[11] F.Q. Liu, G.Q. Lu, C.Y. Wang, J. Electrochem. Soc. 153 (2006) A543.
[12] X. Ren, T.E. Springer, S. Gottesfeld, J. Electrochem. Soc. 147 (2000) 92.
[13] G.J.M. Janssen, M.L.J. Overvelde, J. Power Sources 101 (2001) 117.
[14] D.R. Sena, E.A. Ticianelli, V.A. Paganin, E.R. Gonzalez, J. Electroanal. Chem. 477 (1999) 164.
[15] Z. Qi, A. Kaufman, J. Power Sources 109 (2002) 38.
[16] N. Rajalakshmi, T.T. Jayanth, R. Thangamuthu, G. Sasikumar, P. Sridhar, K.S. Dhathathreyan, Int. J. Hydrogen Energy 29 (2004) 1009.
[17] T. Mennola, M. Noponen, T. Kallio, M. Mikkola, T. Hottinen, J. Appl. Electrochem. 34 (2004) 31.
[18] S.S. Sandhu, R.O. Crowther, J.P. Fellner, Electrochim. Acta 50 (2005) 3985.
[19] M.G. Izenson, R.W. Hill, J. Fuel Cell Sci. Tech. 2 (2005) 1.
[20] Y. Cai, J. Hu, H. Ma, B. Yi, H. Zhang, Electrochim. Acta 51 (2006) 6361.
[21] S. Ge, B. Yi, P. Ming, J. Electrochem. Soc. 153 (2006) A1443.
[22] J.P.G. Villaluenga, B. Seoane, V.M. Barragán, C. Ruiz-Bauzá, J. Membrane Sci. 274 (2006) 116.
[23] S. Ge, X. Li, B. Yi, I.-M. Hsing, J. Electrochem. Soc. 152 (2005) A1149.
[24] T. Schaffer, T. Tschinder, V. Hacker, J.O. Besenhard, J. Power Sources 153 (2006) 210.
[25] T. Murahashi, M. Naiki, E. Nishiyama, J. Power Sources 162 (2006) 1130.
[26] B.S. Pivovar, Polymer 47 (2006) 4194.
[27] J. St-Pierre, J. Electrochem. Soc. 154 (2007) B88.
[28] C. Lim, C.Y. Wang, Electrochim. Acta 49 (2004) 4149.
[29] G. Lin, T.V. Nguyen, J. Electrochem. Soc. 152 (2005) A1942.
[30] T. Schultz, K. Sundmacher, J. Membrane Sci. 276 (2006) 272.

[31] S.U. Jeong, E.A. Cho, H.J. Kim, T.H. Lim, I.H. Oh, S.H. Kim, J. Power Sources 159 (2006) 1089.
[32] Q. Yan, H. Toghiani, J. Wu, J. Power Sources 158 (2006) 316.
[33] C.Y. Wang, Chem. Rev. 104 (2004) 4727.
[34] U. Pasaogullari, C.Y. Wang, J. Electrochem. Soc. 151 (2004) A399.
[35] X. Ren, T.E. Springer, T.A. Zawodzinski, S. Gottesfeld, J. Electrochem. Soc. 147 (2000) 466.
[36] S.Q. Song, Z.X. Liang, W.J. Zhou, G.Q. Sun, Q. Xin, V. Stergiopoulos, P. Tsiakaras, J. Power Sources 145 (2005) 495.
[37] C. Xu, T.S. Zhao, Q. Ye, Electrochim. Acta 51 (2006) 5524.